

Molecular Complex Formation between Riboflavin and Salicylate in an Aqueous Medium

Silpi Datta, Chaitali Mukhopadhyay, and Swapan Kumar Bose*

Department of Chemistry, University of Calcutta, 92, A.P.C. Road, Kolkata-700 009, India

Received March 6, 2003; E-mail: chaitalicu@yahoo.com

Evidence for an intermolecular interaction of riboflavin and sodium salicylate in an aqueous medium was obtained from the presence of isosbestic points in the absorption spectra and an isoemissive point in the emission spectra. The equilibrium constant was estimated from absorption and emission studies, and also from the solubility of riboflavin in an aqueous solution of sodium salicylate, and was found to be in the range of 10–14 mol dm⁻³. Lifetime measurements indicate a predominantly static mechanism of quenching. The Stern–Volmer constant for the quenching of riboflavin by sodium salicylate was significantly reduced upon the addition of urea. An MD simulation study on the system revealed a stacked conformation, which is probably due to a hydrophobic interaction of the two components.

The term flavin refers to a generic set of compounds containing the heterocyclic isoalloxazine chromophore. They are very versatile compounds and are involved in a host of biological processes.¹ In aerobic metabolic processes, they catalyze two-electron dehydrogenations of different substrates, and participate in one-electron transfers to various metal centers.¹ They are cofactors of the flavoenzymes, which are ubiquitous and can catalyze a wide variety of chemical reactions essential for sustaining the living conditions of each organism.² The mechanism of cofactor (i.e. flavins) binding by the flavoenzymes involve a stacking interaction between a conserved aromatic residue (e.g., tyrosine, tryptophan or histidine) at the cofactor binding site and the isoalloxazine ring of the flavin. This has been observed in the cases of the flavoenzyme, ferredoxin-NADH reductase, where the isoalloxazine ring of flavin is stabilized by a stacking interaction with the Tyr 303 residue.³ In the crystal structure of D-amino acid oxidase-*o*-amino benzoate complex, a similar interaction between the flavin and the aromatic ring of the Tyrosine 224 residue is observed at the binding site.¹ Flavodoxin reductase, on the other hand, contains Trp 248 at the cofactor binding site.⁴ In flavoenzymes that do not have a bound cofactor, e.g., NAD(P)H: Flavin oxidoreductase from *E. coli*, do not have such an aromatic residue at the cofactor binding site.⁴ Thus, the stacking interaction appears to be important in stabilizing the cofactor in the bound form.

Stacking interaction is important in the functioning of the flavoenzymes, where the substrates containing an aromatic ring system gain additional stability in the binding site upon stacking onto the flavin cofactor. One of the earliest known flavoenzyme is ‘Old Yellow Enzyme’, obtained from yeast. Although the exact physiological function of this enzyme is not known, many studies have been conducted with this enzyme because of its ability to form beautiful charge transfer complexes with aromatic and heteroaromatic compounds containing an ionizable hydroxy group. The crystal structure of

the enzyme with bound phenol clearly shows that a parallel stacking of flavin and phenol is required for the observed charge-transfer interaction.² A stacking interaction between Trp 27 and the isoalloxazine ring of flavin forms the structural basis of the binding of riboflavin to the *Schizosaccharomyces pombe* 6,7-dimethyl-8-ribityllumazine synthase.⁵

Thus, the interaction of the flavin moiety with aromatic ring systems appears to be a vital factor in stabilizing it as a cofactor as well as in the functioning of many flavoenzymes. In order to understand the nature of this interaction we chose a model system comprising of riboflavin and a salicylate anion, and characterized the interaction in an aqueous medium. Riboflavin, vitamin B₂, is a water-soluble, yellow, fluorescent compound, which functions as a coenzyme in numerous redox reactions in metabolic pathways and in energy production. Salicylic acid, on the other hand, is one of the most widely used drugs with analgesic and antipyretic activity. Studies have suggested that salicylic acid may serve as one-electron-donating substrates for catalases/peroxidases.⁶ Studies on the interaction of flavin derivatives with salicylic acid and its derivatives in a non-aqueous medium, such as chloroform and benzene, were reported earlier. In these studies, a hydrogen-bonding interaction between salicylic acid and riboflavin has been suggested.⁷ Riboflavin and salicylic acid form a 1:1 cyclic hydrogen-bonded dimer through the N-3 proton and the C-2 carbonyl oxygen of the isoalloxazine ring of RF and the carboxylic hydroxy proton and carbonyl oxygen of SA in an aprotic solvent.⁷ The optimum hydrogen-bonding requires that RF and SA be placed side-by-side, so that the arrangement of the donor and acceptor groups is linear. Since these studies have been made in aprotic solvents, stacking interactions between flavins and salicylic acid have not been emphasized. We have studied the binding of riboflavin to salicylic acid in an aqueous medium. It is quite conceivable that in an aqueous medium a stacking interaction will be crucial rather than hydrogen-bonding.

Experimental

Materials and Methods. Riboflavin (RF) was purchased from Sigma Chemicals Co. AR-grade salicylic acid (SA) was obtained from S.D. fine-chem Ltd. (India). GR-quality sodium salicylate (NAS), urea, potassium nitrate (KNO_3) and potassium iodide (KI) were obtained from E. Merck (India). AR-grade sodium dihydrogenorthophosphate and disodium hydrogenorthophosphate were obtained from Qualigens Fine Chemicals (India). Water distilled twice in an all glass apparatus was used for preparing all solutions.

The UV-visible absorption spectra were recorded using a Hitachi U-3501 spectrophotometer with 1 cm quartz cuvettes. The concentration of RF used for absorption experiments with NAS was $5 \times 10^{-5} \text{ mol dm}^{-3}$. The range of the NAS used was $(0.0125\text{--}0.4) \text{ mol dm}^{-3}$. A phosphate buffer $(0.10 \text{ mol dm}^{-3})$ was used for maintaining pH values of 6, 7, and 8. The pH of the solutions was measured by an Elico LI127 pH meter.

The fluorescence spectra were recorded on a Perkin-Elmer LS50B emission spectrofluorimeter. The concentration of the RF used for all steady state fluorescence experiments was of the order of $10^{-5} \text{ mol dm}^{-3}$. For the quenching of RF by KI in the presence of salicylic acid, the KI concentration was varied from $(1\text{--}7) \text{ mmol dm}^{-3}$ and that of salicylic acid was $(1.7\text{--}13.6) \text{ mmol dm}^{-3}$. For the quenching of RF by NAS, the concentration range for NAS was $(1\text{--}8) \text{ mmol dm}^{-3}$ in the presence of 0.10 (M) phosphate buffers of pH 6, 7, and 8. The effect of the ionic strength on the fluorescence spectra were studied by repeating the fluorescence quenching experiments of RF by NAS in a medium of $0.20 \text{ mol dm}^{-3} \text{ KNO}_3$ at pH 6.0. The fluorescence quenching experiments were studied using excitation wavelengths of 350 nm and 440 nm with both excitation and emission slit widths of 5.0 nm. The peaks of RF and NAS were monitored at 522 nm and 412 nm, respectively. The absorption and emission experiments of the RF-NAS pair were repeated in the presence of varying amounts of urea at a concentration of $(1\text{--}5) \text{ mol dm}^{-3}$ at pH 6.0. The temperatures for the absorption and emission experiments were maintained within $22\text{--}26^\circ\text{C}$.

Solubility experiments were performed by saturating solutions of NAS ranging between $(0\text{--}8) \text{ mmol dm}^{-3}$ with RF in the presence of $0.2 \text{ mol dm}^{-3} \text{ KNO}_3$ at pH 6.0 using a magnetic stirrer, and filtering. Two mL of the filtrate was diluted to 10 mL and the absorbance was noted at 450 nm using 1 cm cuvettes. Fluorescence lifetimes were determined from total emission intensity decay measurements using a time-domain assembled fluorimeter with components from Edinburgh Analytical Instruments and EG&GORTEC, and operated in the time-correlated single-photon counting mode. Excitation was provided by a pulsed high-pressure 152 kPa N_2 lamp operating at 1.3 ns. The RF was excited at 380 nm and the emission decay profile was monitored at 522 nm. The time-resolved measurements were performed with 10^{-4} (M) RF collecting 5000 photon counts in the peak channel. Three different concentrations of NAS (3, 6 and 9 mmol dm^{-3}) were used. All of the solutions were prepared in a medium of 0.03 (M) phosphate buffer of pH 7.5.

For Molecular Modeling, Insight II software package (Accelrys, Inc., USA, Version 98.0) running on a Silicon Graphics O2 workstation was used. A DISCOVER module⁸ and a CVFF force field were used for molecular mechanics and dynamics calculations. This force field has been used earlier for studying small molecules.⁹ Three-dimensional models of RF and salicylate ion were generated using standard molecular templates. The initial

models were energy minimized to remove any strain. Several initial conformations of the complex of RF and salicylate were generated by keeping the molecules side-by-side within a hydrogen-bonding distance of the C-2 carbonyl and N-3 hydrogen of RF and phenolic OH and carboxylate group of the salicylate anion. After energy minimization of the complex, it was solvated with an 8 Å water layer. The total number of water molecules needed was 315. The solvated complex was energy minimized. A molecular dynamics simulation of the solvated complex was performed for 100 ps after an initial 10 ps equilibration period.

Results and Discussions

Evidence for Complex Formation and Determination of the Equilibrium Constant by an Absorption Method. The absorption spectra of mixtures of RF and salicylic acid showed a decrease in the intensity of both the 445 and 372 nm absorption bands of RF. Since the solubility of salicylic acid in water is very low, NAS was used in place of salicylic acid for a quantitative analysis of the intensities of the RF bands. The absorption spectra of mixtures of RF and NAS (Fig. 1) showed a decrease in the intensity of the two RF bands upon increasing the concentration of NAS for a fixed RF concentration and pH. Three isosbestic points were discerned in the absorption spectra of the mixtures. This is indicative of a complex formation between RF and NAS. The decreased absorbance values recorded at 445 and 490 nm were used to calculate the equilibrium constants, K . These two wavelengths were selected because they are well removed from the isosbestic points.

The equilibrium constant of the complex was obtained using the following form of the Benesi-Hildebrand equation:^{10,11}

$$\frac{1}{\Delta A} = \frac{1}{K\Delta\varepsilon} \cdot \frac{1}{C_b^0} + \frac{1}{\Delta\varepsilon}, \quad (1)$$

where ΔA is the difference between the absorbance of the RF solution and that of a mixture containing the same amount of RF and an excess amount of NAS at a fixed pH and an appropriate wavelength. $\Delta\varepsilon$ is the difference between the molar absorptivity of the complex and that of the RF. C_b^0 is the stoichiometric concentration of NAS in the mixture of RF and NAS. A plot of $(\Delta A)^{-1}$ versus $(C_b^0)^{-1}$ is shown in Fig. 2 at two different wavelengths of 445 and 490 nm at pH 6.0.

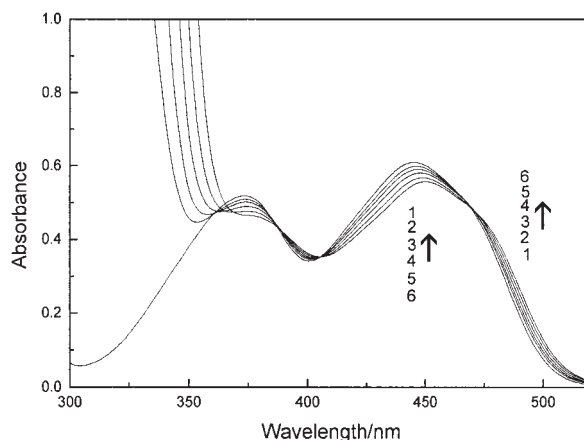


Fig. 1. Effect of NAS on the absorption spectra of RF at pH 6.0. Numbers (1–6) indicate the variation of [NAS] in the order 0, 0.0125, 0.05, 0.10, 0.20, 0.4 mol dm^{-3} .

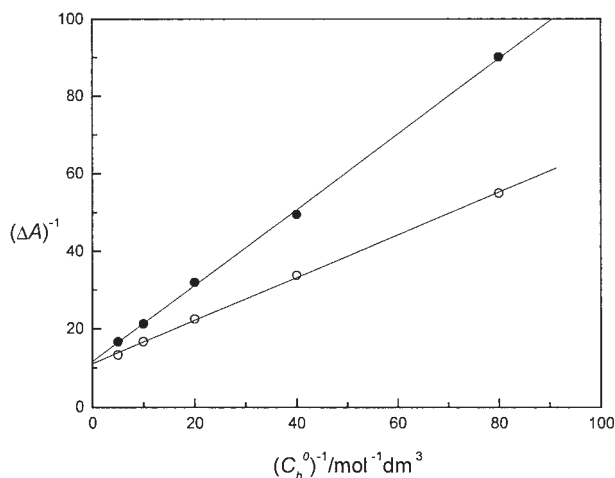


Fig. 2. Plot of $(\Delta A)^{-1}$ versus $(C_b^0)^{-1}$ for the RF–NAS system, pH 6.0 at (i) 445 nm (●) ($r = 0.99969$), (ii) 490 nm (○) ($r = 0.99962$).

The equilibrium constant values were calculated by taking the ratio of the intercept and the slope of the graph, and were found to lie between $10\text{--}14\text{ mol}^{-1}\text{ dm}^3$ at pH 6, 7 and 8. The K values are pH independent as well as wavelength independent. The close agreement of the K values, determined from two different wavelengths, indicates the presence of a single association complex in aqueous solution. In this context it is worth mentioning that the individual spectrum of RF and NAS are pH independent.

Determination of Complex Formation by Fluorescence Spectroscopy. The Stern–Volmer quenching constants of RF fluorescence by KI were determined at different salicylic acid concentrations. A plot of K_{sv} versus the concentration of salicylic acid is shown in Fig. 3. It was found that K_{sv} decreases with increasing the salicylic acid concentrations, and ultimately reaches a plateau for concentrations higher than 6.0 mmol dm^{-3} . The variation of K_{sv} as a function of the salicylic acid concentration is supporting evidence for complex formation between RF and salicylic acid. The emission spectra for the quenching of RF by NAS at an excitation wave-

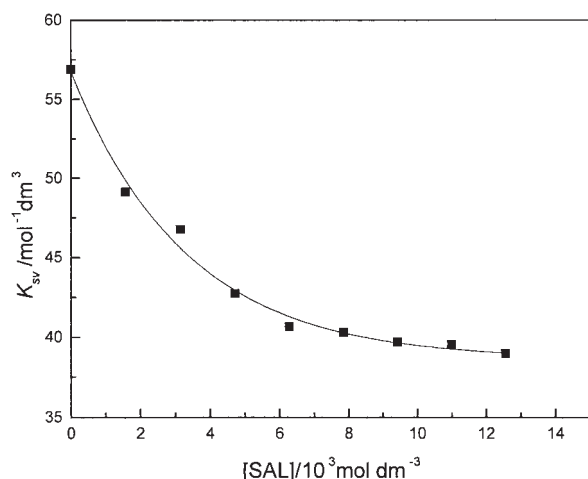


Fig. 3. Effect of salicylic acid on K_{sv} for the quenching of RF fluorescence by KI in aqueous solution.

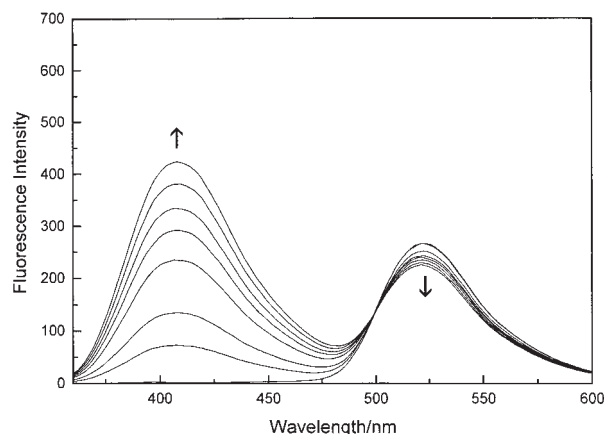


Fig. 4. Emission spectra of RF and NAS at $\lambda_{ex} = 350\text{ nm}$, pH 6.0. Upward \uparrow indicate the variation of [NAS] in the order (1, 2, 3, 4, 5, 6, 7, 8) $\times 10^{-3}\text{ mol dm}^{-3}$ and downward \downarrow indicate the decreasing fluorescence intensity of RF on addition of NAS.

length of 350 nm shows an isoemissive point at 498 nm (Fig. 4). The intensity of the emission maxima of RF at 522 nm for both excitation wavelengths of 350 nm and 440 nm were found to decrease with increasing concentrations of NAS. From the quenching data at two different wavelengths, the K_{sv} values in the range of $(50\text{--}60)\text{ mol}^{-1}\text{ dm}^3$ were obtained. The equilibrium constant, (K) was calculated using

$$\frac{F_0}{\Delta F} = \frac{F_0}{(F_0' - F_0)} + \frac{F_0}{K(F_0' - F_0)} \cdot \frac{1}{C_b^0}, \quad (2)$$

where F_0 , F_0' , and F are the fluorescence intensities of the RF solution, a solution of totally complexed RF with NAS and the experimental solution, respectively. ΔF is the difference in the fluorescence intensities of the RF solution and that of a mixture containing the same amount of RF and varying excess amounts of NAS for a particular excitation wavelength and pH. The above equation was used to find the association constant of lumichrome and β -cyclodextrin.¹² The ratio of the intercept and slope obtained from a plot of $(F_0/\Delta F)$ versus $(C_b^0)^{-1}$ (Fig. 5) gives the value of the equilibrium constant, K . The K values obtained at two different wavelengths of 350 nm and 440 nm are almost identical, and range between $(45\text{--}55)\text{ mol}^{-1}\text{ dm}^3$. This indicates that a similar quenching mechanism is involved in both cases. The K values are almost equal to the K_{sv} values at these two wavelengths. However, the K values obtained here are significantly higher than those obtained from absorption experiments.

The disparity in the K values obtained from fluorescence quenching and absorption experiments may have been due to the effect of the ionic strengths of the solutions used. The ionic strength of the NAS solution used in the absorption method is much higher than that used in the fluorescence quenching experiments. The fluorescence quenching experiments were repeated in a medium of $0.20\text{ mol dm}^{-3}\text{ KNO}_3$ at pH 6.0. This particular concentration of KNO_3 is the average of the concentration range of NAS used in the absorption experiments. In this medium of increased ionic strength, the equilibrium constant, (K) was reduced to 14 mol dm^{-3} [Figure not shown]. This is in fair agreement with those obtained from absorption

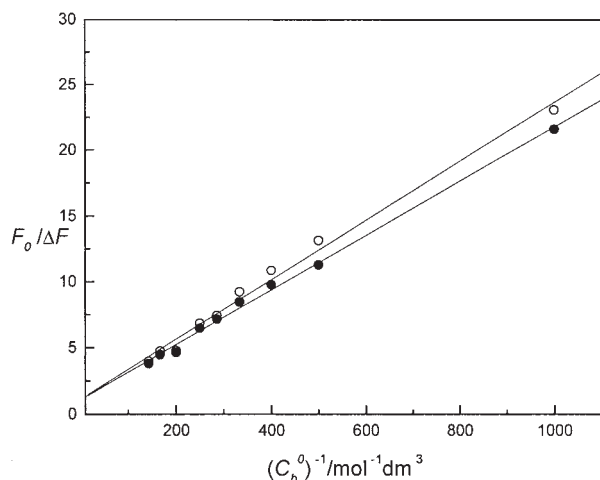


Fig. 5. Plot of $(F_0/\Delta F)$ versus $(C_b^0)^{-1}$ for the RF-NAS system, pH 6.0 at (i) 350 nm (●) ($r = 0.9981$), (ii) 440 nm (○) ($r = 0.99537$).

studies. The reduction of K with an increase in the ionic strength indicates that the association complex is a charged species.

Determination of Mechanism of Quenching by Lifetime Measurements. To substantiate the mechanism of quenching, fluorescence lifetime measurements were carried out. All of the decay curves were found to fit a single exponential decay function, which is shown in Fig. 6. The fluorescence lifetimes (τ) of RF were 4.00 ns, 4.20 ns, 4.40 ns for NAS concentrations of 3, 6, and 9 mmol dm⁻³, respectively, and that for RF in absence of NAS was 4.63 ns, very close to the previously reported value of 4.64 ns.¹³ The change in the τ values obtained upon the addition of NAS is marginal, and can be considered to be insignificant. This indicates that the above quenching mechanism is predominantly static, the dynamic quenching involved being negligible.

Determination of the Equilibrium Constant by the Solubility Method. The solubility of RF in water was found to increase considerably in the presence of NAS. For determining the equilibrium constants by solubility methods, a series of

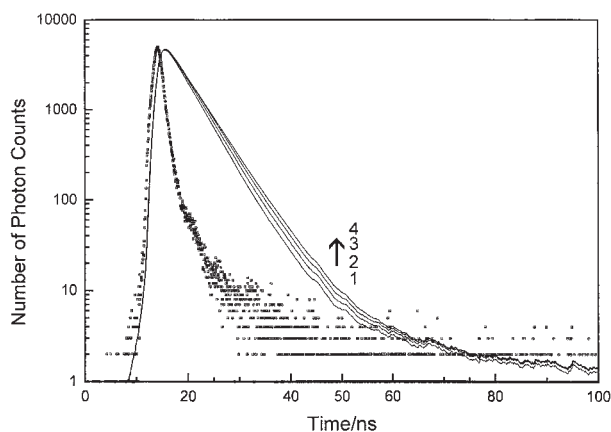


Fig. 6. Single exponential fits to the fluorescence intensity decay profiles of RF in (1) aqueous solution and in presence of (2) 3 mmol dm⁻³, (3) 6 mmol dm⁻³, and (4) 9 mmol dm⁻³ NAS.

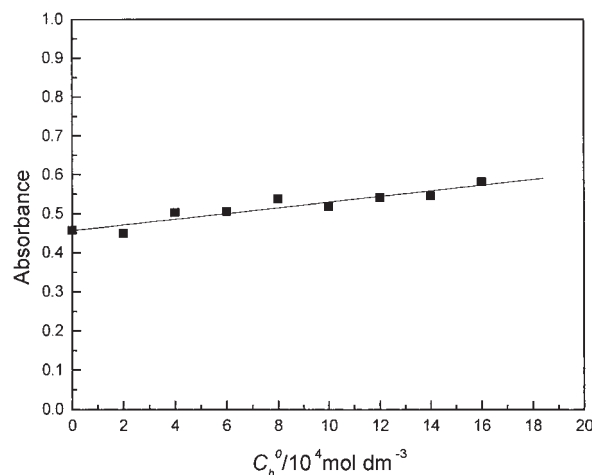


Fig. 7. Plot for the solubility of RF in aqueous solution of NAS at pH 6.0 in presence of 0.20 mol dm⁻³ KNO₃ ($r = 0.93972$).

solutions of NAS were taken in the presence of phosphate buffer of pH 6.0 and 0.20 mol dm⁻³ KNO₃. The solubilities of RF in these solutions were determined according to a procedure described in the Materials and Methods section. The absorbances for the above-mentioned solutions at 450 nm were processed using the following equation:¹²

$$A_{\text{mix}} = A_{\text{RF}} + K A_{\text{RF}} C_b^0, \quad (3)$$

where A_{mix} and A_{RF} are the absorbances of the complexed RF and RF in an aqueous solution respectively. C_b^0 is the stoichiometric concentration of NAS. The plot of A_{mix} versus C_b^0 (Fig. 7) is linear. From the ratio of the slope and intercept of the curve, an equilibrium constant of 12 mol dm⁻³ was obtained which, is in close agreement with the K values obtained from absorption methods. The presence of any hydrotropic effect is ruled out because the concentration range of the NAS used was much lower than that required for a hydrotropic effect.¹⁴

Effect of Urea on the Absorption and Fluorescence Spectra. Urea is a well-known chemical denaturant for proteins, and at concentrations above 6–8 M, destroys the tertiary structure of proteins. Although the exact mechanism by which urea destroys the protein tertiary structure is not known, several proposals have been made which include a breakdown of the water structure by urea,¹⁵ preferential solvation of hydrophobic residues,¹⁵ as well as adsorption onto the surface residues, leading to the swelling of protein, and finally denaturation.¹⁵ To test whether urea can break the complex formed between RF and NAS in an aqueous medium, the effects of urea on the absorption and fluorescence spectra of RF and NAS were studied. The absorption spectra of a mixture of RF (10⁻⁵ mol dm⁻³) and NAS (0.20 mol dm⁻³) in the presence of varying concentrations of urea at pH 6.0 are shown in Fig. 8. The two absorption bands of RF at 445 and 372 nm were found to increase in intensity with respect to the spectra for the mixture of RF and NAS in absence of urea, the more significant change being observed in the case of the 372 nm band. Fluorescence-quenching experiments of RF by NAS were repeated in the presence of varying urea concentrations at pH 6.0. A plot of

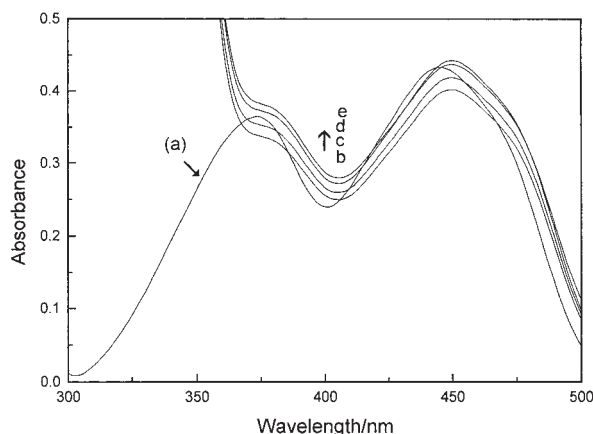


Fig. 8. Effect of urea on the absorption spectra of a mixture of RF ($5 \times 10^{-2} \text{ mol dm}^{-3}$) and NAS (0.20 mol dm^{-3}), labels b, c, d, e indicating the varying urea concentrations 0 mol dm^{-3} , 1 mol dm^{-3} , 2 mol dm^{-3} , 4 mol dm^{-3} and 'a' indicating spectra of pure RF.

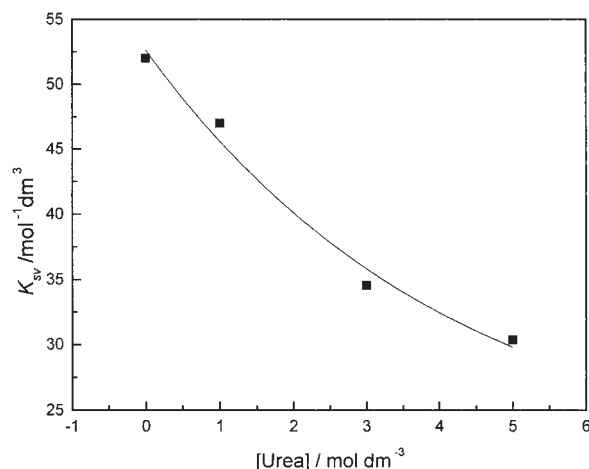


Fig. 9. Effect of urea on K_{sv} for the quenching of RF fluorescence by NAS at pH 6.0.

K_{sv} as a function of the urea concentration is shown in Fig. 9. The K_{sv} value decreases with increasing urea concentrations, ultimately reaching a constant value of about $30 \text{ mol}^{-1} \text{ dm}^3$ at higher concentrations of urea. However, absorption and emission spectra of RF and NAS separately remains unaffected in the presence of urea.

In a non-aqueous medium, a hydrogen-bonding mechanism was proposed earlier⁷ for the formation of an association complex between flavins and small organic molecules. In an aqueous medium, however, other mechanisms, e.g., stacking interactions, charge transfer, etc., may be important for complex formation. The changed absorption spectra as well as the reduction of the K_{sv} values with increasing urea concentrations indicate that the RF–NAS interaction is weakened in the presence of urea. Although the K_{sv} value is reduced, it does not become insignificantly small. This indicates that interactions, which are unaffected by urea, might also be operative. We suggest a charge-transfer mechanism between the salicylate anion as a donor and the RF as an acceptor was observed for the RF– NaN_3 pair¹⁶ where the association constant was calcu-

lated to be as low as 4 mol dm^{-3} . The association constants in the order of $300\text{--}400 \text{ mol dm}^{-3}$, as reported in the literature for flavin–substrate systems in a non-aqueous medium, involved hydrogen-bonding interactions. It was reported that the sites of RF involved in that interaction were the C-2 carbonyl oxygen and the N-3 proton. In this work, a low association constant signifies a weaker interaction.

Molecular Modeling. One of the two starting conformations chosen for the RF–NAS complex had the N-3 hydrogen atom placed within the hydrogen-bonding distance of the carboxylic group of the salicylate anion, while the other had the C-2 carbonyl oxygen placed near to the phenolic OH group. During MD simulations, however, the salicylate anion moved away from the side-by-side position within the equilibration period, itself, and became stacked onto the isoalloxazine ring of RF with an average distance of (4–5) Å between the aromatic ring of SA and the heteroaromatic rings of RF, and remained in that position throughout the entire simulation time. This indicates that in the presence of water the stacked complex is more favourable than the side-by-side complex. It is conceivable that the van der Waals interaction will be more favourable in the stacked form than in the side-by-side form. Also, in presence of water, RF and NAS can form hydrogen bonds with water molecules instead of forming the inter-molecular hydrogen bonds needed to stabilize the side-by-side complex. Thus, water might play a crucial role in stabilizing the stacked form of the complex. The diagram (Fig. 10) shows the stacked conformation of the complex. From the trajectory-averaged conformation of the complex, it was observed that the stacking interaction of the hydrophobic rings of RF and NAS as well as the electrostatic interaction between the phenolic OH and the carboxylate groups of salicylate anion and the C-2 carbonyl oxygen and the N-3 hydrogen of RF are crucial for stabilizing the complex.

Experimental evidence confirms the formation of a complex between riboflavin and sodium salicylate. The association-constant value for the formation of a complex obtained from different experimental methods gave a consistent value, and its magnitude was in the range of $10\text{--}14 \text{ mol dm}^{-3}$. In an aqueous solution, the low association constant is indicative of the formation of a weak complex; whereas the association

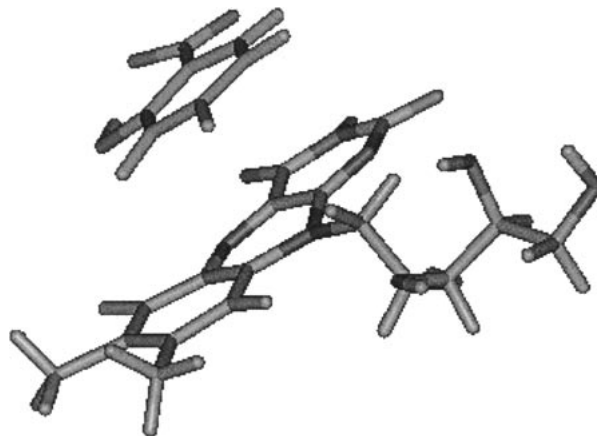


Fig. 10. Trajectory averaged structure of the interaction of RF and NAS.

constant obtained for the same system under aprotic conditions is very high, indicating a stronger interaction in a non-polar environment. The presence of urea, a known structure breaker, weakens the binding of the RF–NAS complex. Molecular modeling studies also indicate the presence of a stacked complex.

The authors gratefully acknowledge Prof. S. Basak, Chemical Sciences Division, Saha Institute of Nuclear Physics, Kolkata for providing the facilities for fluorescence lifetime measurements. S.D. acknowledges University of Calcutta for financial assistance.

References

- 1 R. Miura, *Chem. Rec.*, **1**, 183 (2001).
- 2 V. Massey, *Biochem. Soc. Trans.*, **28**, 283 (2000).
- 3 J. A. Hermoso, T. Mayoral, M. Faro, C. Gomez-Moreno, J. Sanz-Aparicio, and M. Medina, *J. Mol. Biol.*, **319**, 1133 (2002).
- 4 T. M. Louie, H. Yang, P. Karnchanaphanurach, and X. S. Xie, *J. Biol. Chem.*, **277**, 39450 (2002).
- 5 S. Gerhardt, I. Haase, S. Steinbacher, J. T. Kaiser, M. Cushman, A. Bacher, R. Huber, and M. Fischer, *J. Mol. Biol.*, **318**, 1317 (2002).
- 6 J. Durner and D. F. Klessig, *J. Biol. Chem.*, **271**, 28492 (1996).
- 7 B. S. Yu, S. J. Lee, S. J. Lee, and H. H. Chung, *J. Pharm. Sci.*, **72**, 592 (1983).
- 8 Discover Manual, Version 98.0.
- 9 C. Mukhopadhyay, *Biopolymers*, **45**, 177 (1998).
- 10 H. A. Benesi and J. H. Hildebrand, *J. Am. Chem. Soc.*, **71**, 270 (1949).
- 11 P. Douglas, G. Waechter, and A. Mills, *Photochem. Photobiol.*, **52**, 473 (1990).
- 12 B. Sarkar, U. Das, S. Bhattacharya, and S. K. Bose, *Bull. Chem. Soc. Jpn.*, **68**, 1807 (1995).
- 13 K. Bystra-Mieloszyk, A. Balter, and R. Drabent, *Photochem. Photobiol.*, **41**, 141 (1985).
- 14 R. E. Coffman and D. O. Kildsig, *J. Pharm. Sci.*, **85**, 951 (1996).
- 15 A. Wallqvist, D. G. Covell, and D. Thirumalai, *J. Am. Chem. Soc.*, **120**, 427 (1998).
- 16 B. Sarkar, U. Das, S. Bhattacharya, and S. K. Bose, *J. Chem. Res., Synop.*, **72**, 123 (1995).